Communication

Low-Temperature Polyol Synthesis of AuCuSn and AuNiSn: Using Solution Chemistry to Access Ternary Intermetallic Compounds as Nanocrystals

Brian M. Leonard, Nattamai S. P. Bhuvanesh, and Raymond E. Schaak

J. Am. Chem. Soc., **2005**, 127 (20), 7326-7327• DOI: 10.1021/ja051481v • Publication Date (Web): 03 May 2005

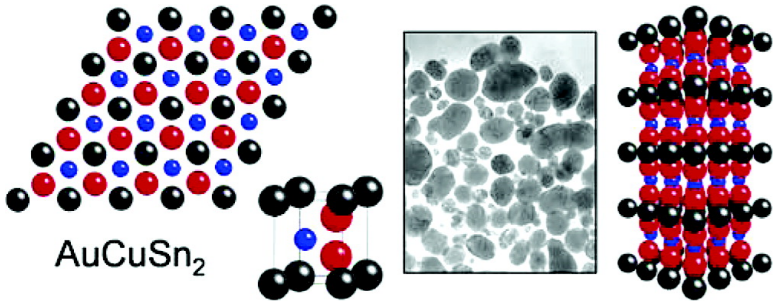

More About This Article

Additional resources and features associated with this article are available within the HTML version:

- Supporting Information
- Links to the 12 articles that cite this article, as of the time of this article download
- Access to high resolution figures
- Links to articles and content related to this article
- Copyright permission to reproduce figures and/or text from this article

View the Full Text HTML

J|A|C|S
COMMUNICATIONS

Published on Web 05/03/2005

Low-Temperature Polyol Synthesis of $AuCuSn_2$ and $AuNiSn_2$: Using Solution Chemistry to Access Ternary Intermetallic Compounds as Nanocrystals

Brian M. Leonard, Nattamai S. P. Bhuvanesh, and Raymond E. Schaak*

Department of Chemistry, Texas A&M University, College Station, Texas 77842-3012

Received March 8, 2005; E-mail: schaak@mail.chem.tamu.edu

Ternary intermetallic compounds of the late transition metals possess a wide variety of physical properties, including superconductivity,[1] magnetoresistance,[2] and shape-memory effects,[3] that are important for many scientific studies and technological applications. Traditionally, intermetallics are synthesized using high-temperature arc melting or powder metallurgy techniques, which generally yield thermodynamically stable structures and offer little control over nanostructure and morphology. While a few alternative techniques have been exploited to synthesize new intermetallic phases at low temperatures,[4] solution methods remain largely unexplored. In general, the solvent and surface stabilizing agents can play a key role in kinetically trapping phases that are not stable at high temperatures, providing access to nanocrystalline phases, such as ϵ-Co[5] and wurtzite-type ZnS.[6] This suggests that low-temperature solution strategies, which were recently shown to yield known binary intermetallics,[7] may be attractive for synthesizing new or metastable intermetallics with more complex structures and compositions.

Here, we show for the first time that low-temperature solution routes originally developed for the synthesis of nanocrystals[8] and nanocrystalline powders[9] can be exploited to access new ordered intermetallics with ternary compositions. While ternary phase diagrams are difficult to map out, the Au−Cu−Sn system has been studied in detail. Intermetallics that form at the solder/metal interface are responsible for the brittleness and fracture of solder joints, and the Au−Cu−Sn system is among the most important for understanding interfacial phase formation in microelectronic devices.[10] While several ternary intermetallics are known in the Au−Cu−Sn system,[11,12] we report the discovery of a new ordered intermetallic compound, $AuCuSn_2$, that is not observed in bulk systems using traditional synthetic techniques.[12] Nanocrystalline $AuCuSn_2$ is stabilized using low-temperature solution chemistry.

$AuCuSn_2$ was synthesized by heating a solution of $HAuCl_4 \cdot 3H_2O$, $Cu(C_2H_3O_2)_2$, $SnCl_2$ (7-fold excess), and poly(vinyl pyrrolidone) (PVP, MW = 40 000) in tetraethylene glycol (TEG, 20 mL) to 70 °C, then adding a freshly prepared solution of dilute $NaBH_4$ and heating the solution to 120−200 °C for 10 min. The X-ray diffraction (XRD) patterns for $AuCuSn_2$ annealed in TEG at 120, 160, and 200 °C are shown in Figure 1a. The patterns, which did not match any known phases in the Au−Cu−Sn ternary system or the constituent unary and binary systems, can be indexed to a hexagonal cell with $a = 4.2287(1)$ Å and $c = 5.2301(1)$ Å. Microprobe analysis indicated an average composition of $Au_{0.80(6)}Cu_{0.98(4)}Sn_{2.0(1)}$, which is close to a nominal composition of $AuCuSn_2$.

Figure 1a shows a simulated powder XRD pattern for NiAs-type $AuCuSn_2$, with Au and Cu disordered over the As site. While the major reflections are in agreement, several smaller reflections in the experimental XRD data are not accounted for. As the Au and Cu atoms are allowed to order in alternating layers, superlattice peaks emerge, and the ordered NiAs superstructure matches all of the observed reflections. The structure was solved in the trigonal space group $P312$, and after imposing additional symmetries, the structure was transformed to the hexagonal space group $P\bar{6}m2$, where the structural model was refined using TOPAS.[13] The calculated diffraction pattern is in good agreement with the experimental data (Figure 2). The structure of $AuCuSn_2$ (Figure 2, inset) consists of an ordered hcp array of Au and Cu in alternating layers with Sn occupying the octahedral holes. Refinement of the atomic positions indicated only 10% disorder between the Au and Cu sites. Importantly, a previous study of the Au−Cu−Sn phase diagram under equilibrium conditions reported that $AuCuSn_2$ exists as a *disordered* NiAs-type solid solution at 250 °C.[12] In contrast, we find that the *ordered* structure is stable at 250 °C when the polyol method is used, providing strong evidence that low-temperature solution routes can stabilize structures that do not form using traditional synthetic techniques.

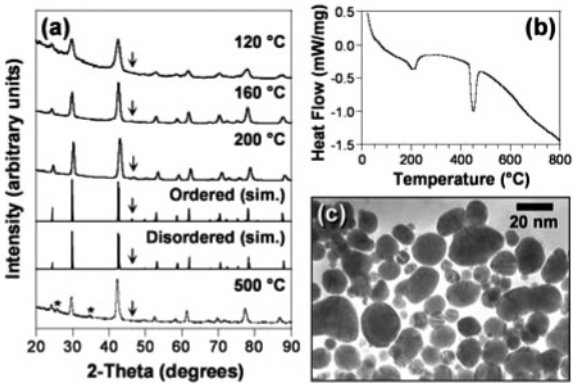

Figure 1. (a) Powder XRD patterns for $AuCuSn_2$ synthesized in TEG at 120, 160, and 200 °C, simulated XRD data for ordered and disordered (NiAs-type) $AuCuSn_2$, and $AuCuSn_2$ powder heated to 500 °C under Ar; (b) DSC trace and (c) TEM micrograph of $AuCuSn_2$ nanocrystals synthesized at 160 °C in TEG and re-suspended in ethanol. The arrows in (a) highlight a superlattice peak (see Supporting Information for others), and asterisks show a small amount of SnO_2 that crystallizes on heating.

The differential scanning calorimetry (DSC) data in Figure 1b show two endotherms. The first, near 210 °C, corresponds to the melting of Sn. A small Sn impurity was included in the structure refinement shown in Figure 2, and magnetic susceptibility measurements indicated a superconducting transition at 3.7 K, consistent with a small Sn impurity. The endotherm at 450 °C is evidence of an order/disorder phase transition, which is confirmed by powder XRD data for $AuCuSn_2$ heated to 500 °C under Ar (Figure 1a), showing the disappearance of the superlattice reflections. Mechanistic details of phase formation and stability under different conditions will be addressed in future work.

Figure 1c shows a transmission electron micrograph (TEM) of $AuCuSn_2$ synthesized at 160 °C, indicating that the new ordered phase exists as well-defined nanocrystals. The average crystallite size determined by analysis of TEM micrographs (ca. 180 nano-

10.1021/ja051481v CCC: $30.25

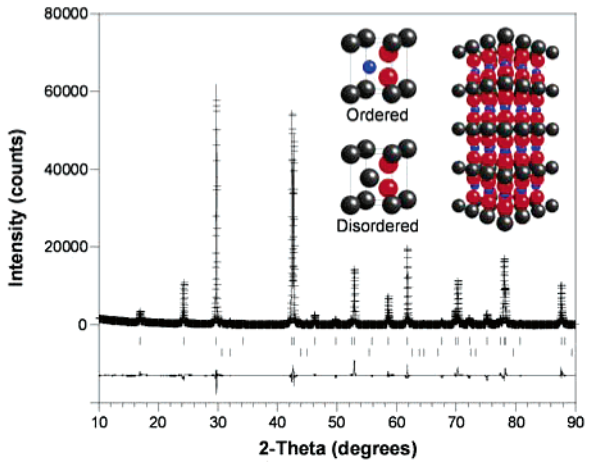

Figure 2. Rietveld structure refinement for $AuCuSn_2$ synthesized at 200 °C in TEG showing the calculated (top, solid line) and observed (top, crosses) XRD patterns. The difference curve (bottom, solid line) indicates the agreement between the observed and calculated patterns. The top and bottom sets of tick marks indicate the allowed Bragg reflections for ordered $AuCuSn_2$ and a Sn impurity, respectively. The refinement yielded R_{exp} = 3.28%, R_{wp} = 13.60%, and R_p = 9.31%. Inset: Structure of ordered $AuCuSn_2$ and unit cells for the ordered and disordered structures. (Au = gray, Cu = blue, Sn = red. Gray spheres in the disordered structure represent a mixture of Au and Cu.)

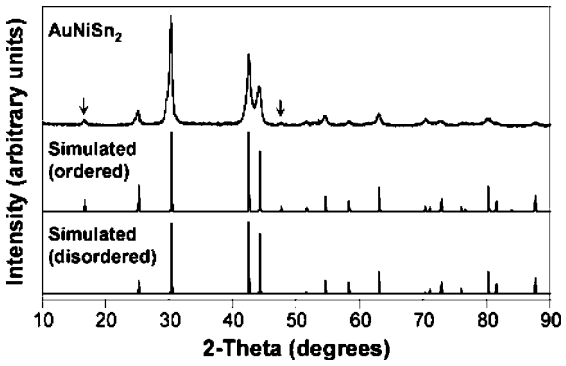

Figure 3. Observed and simulated (ordered and disordered) powder XRD patterns for $AuNiSn_2$, with a = 4.093(1) Å and c = 5.301(1) Å. Primary superlattice reflections are marked with an arrow. The average particle size was estimated to be 12 nm using the Scherrer equation.

crystals) is 27 ± 14 nm. No attempt was made at this point to control the size or dispersity of the nanocrystals, although we expect that standard synthetic modifications to the polyol process will allow such control in the future.

Using the same solution method, ordered $AuNiSn_2$ can also be synthesized. Like $AuCuSn_2$, $AuNiSn_2$ is stabilized at low temperatures in solution and was not identified in previous studies of the ternary phase diagram.[14] Figure 3 shows the powder XRD pattern for nanocrystalline $AuNiSn_2$ and the simulated XRD data for the ordered and disordered structures based on the refined structural model for $AuCuSn_2$. Magnetic susceptibility data for $AuNiSn_2$ indicate only a small paramagnetic impurity.

The discovery of a new family of ordered intermetallics as nanocrystals using low-temperature solution methods has several important implications. First, it shows that ternary intermetallic phases are accessible as nanocrystals, which has the potential to greatly expand the availability of complex multimetallic nanomaterials for future studies of size-dependent properties, intermetallic catalysis, and integration into nanotechnological devices. Second, it demonstrates that low-temperature solution methods that have been developed for nanocrystal synthesis are appropriate exploratory media for synthesizing new and possibly metastable intermetallics. Third, it opens the door to studying phase formation and stability of complex multimetallic solids at low temperatures, where reaction kinetics are typically too slow and impurities are unavoidable. Finally, the fact that we were able to discover new phases in well-studied ternary systems attests to the ability of this solution-based synthetic method to stabilize new structures that are not accessible using traditional methods. We expect that other new binary, ternary, and perhaps quaternary intermetallic compounds will be accessible as nanocrystalline solids using this approach.

Acknowledgment. This work was supported by startup funds from Texas A&M University and funding from the Robert A. Welch Foundation (Grant No. A-1583). Acknowledgment is made to the donors of the Petroleum Research Fund, administered by the American Chemical Society, for partial support of this work. The electron microprobe was partially funded by the DOE. The SQUID magnetometer was obtained with funds provided by an equipment grant from the NSF. Electron microscopy was performed at the Microscopy and Imaging Center at Texas A&M University.

Supporting Information Available: Experimental procedure and characterization details; larger version of experimental and simulated XRD data for $AuCuSn_2$; crystallographic and magnetic data. This material is available free of charge via the Internet at http://pubs.acs.org.

References

(1) (a) Khan, H. R.; Trunk, H.; Raub, Ch. J.; Fertig, W. A.; Lawson, A. C. *J. Less-Common Met.* **1973**, *30*, 167−168. (b) He, T.; Huang, Q.; Ramirez, A. P.; Wang, Y.; Regan, K. A.; Rogado, N.; Hayward, M. A.; Haas, M. K.; Slusky, J. S.; Inumara, K.; Zandbergen, H. W.; Ong, N. P.; Cava, R. J. *Nature* **2001**, *411*, 54−56.

(2) Van Dover, R. B.; Gyorgy, E. M.; Cava, R. J.; Krajewski, J. J.; Felder, R. J.; Peck, W. F. *Phys. Rev. B* **1993**, *47*, 6134−6137.

(3) Ullakko, K.; Huang, J. K.; Kantner, C.; O'Handley, R. C.; Kokorin, V. V. *Appl. Phys. Lett.* **1996**, *69*, 1966−1968.

(4) (a) Perepezko, J. H. *Mater. Sci. Eng.* **1984**, *65*, 125−135. (b) Suryanarayana, C. *Prog. Mater. Sci* **2001**, *46*, 1−184. (c) Chen, X. Z.; Larson, P.; Sportouch, S.; Brazis, P.; Mahanti, S. D.; Kannenwurf, C. R.; Kanatzidis, M. G. *Chem. Mater.* **1999**, *11*, 75−83. (d) Latturner, S. E.; Kanatzidis, M. G. *Inorg. Chem.* **2004**, *43*, 2−4. (e) Noh, M.; Thiel, J.; Johnson, D. C. *Science* **1995**, *270*, 1181−1184. (f) Noh, M.; Johnson, C. D.; Hornbostel, M. D.; Thiel, J.; Johnson, D. C. *Chem. Mater.* **1996**, *8*, 1625−1635.

(5) Dinega, D. P.; Bawendi, M. G. *Angew. Chem., Int. Ed.* **1999**, *38*, 1788−1791.

(6) Zhao, Y.; Zhang, Y.; Zhu, H.; Hadjipanayis, G. C.; Xiao, J. Q. *J. Am. Chem. Soc.* **2004**, *126*, 6874−6875.

(7) (a) Sra, A. K.; Schaak, R. E. *J. Am. Chem. Soc.* **2004**, *126*, 6667−6672. (b) Sra, A. K.; Ewers, T. D.; Schaak, R. E. *Chem. Mater.* **2005**, *17*, 758−766. (c) Schaak, R. E.; Sra, A. K.; Leonard, B. M.; Cable, R. E.; Bauer, J. C.; Han, Y.-F.; Means, J.; Teizer, W.; Vasquez, Y.; Funck, E. S. *J. Am. Chem. Soc.* **2005**, *127*, 3506−3515.

(8) Cushing, B. L.; Kolesnichenko, V. L.; O'Connor, C. J. *Chem. Rev.* **2004**, *104*, 3893−3946.

(9) Fievet, F.; Lagier, J. P.; Blin, B.; Beaudoin, B.; Figlarz, M. *Solid State Ionics* **1989**, *32*−*33*, 198−205.

(10) Roeder, J. F.; Notis, M. R.; Goldstein, J. I. *Defect Diffus. Forum* **1988**, *59*, 271−278.

(11) (a) Karlsen, O. B.; Kjekshus, A.; Rost, E. *Acta Chem. Scand.* **1990**, *44*, 197−198. (b) Peplinski, B.; Zakel, E. *Mater. Sci. Forum* **1994**, *166*−*169*, 443−448.

(12) Karlsen, O. B.; Kjekshus, A.; Rost, E. *Acta Chem. Scand.* **1992**, *46*, 147−156.

(13) *TOPAS*, version 2.0; General profile and structure analysis software for powder diffraction data; Bruker AXS: Karlsruhe, Germany.

(14) (a) Neumann, A.; Kjekshus, A.; Romming, C.; Rost, E. *J. Solid State Chem.* **1995**, *119*, 142−146. (b) Neumann, A.; Kjekshus, A.; Rost, E. *J. Solid State Chem.* **1996**, *123*, 203−207.

JA051481V